Data in Brief 19 (2018) 2291–2296

Contents lists available at ScienceDirect

Data in Brief

journal homepage: www.elsevier.com/locate/dib

Data Article

# Dataset on aerosol loading and deposition over Nouakchott-Mauritania

M.E. Emetere [*,a,c], G.A. Adeyemi [b]

[a] Department of Physics, Covenant University Canaan Land, P.M.B 1023, Ota, Nigeria
[b] Department of Civil Engineering, Covenant University Canaan Land, P.M.B 1023, Ota, Nigeria
[c] Department of Mechanical Engineering and Science, University of Johannesburg, APK, South Africa

ARTICLE INFO

*Article history:*
Received 9 June 2018
Received in revised form
1 July 2018
Accepted 5 July 2018
Available online 9 July 2018

*Keywords:*
Air pollution
Aerosol
Nouakchott
Mauritania
Model

ABSTRACT

Aerosol optical depth (AOD) is a vital parameter that determines air quality over a geographic enclave. In this paper, the pollution state of Nouakchott-Mauritania was considered. Fifteen years primary (aerosol optical depth) dataset was obtained from the Multi-angle Imaging Spectro-Radiometer (MISR). The secondary datasets were generated from the primary dataset to understand the short and long term effect of aerosol loading over nouakchott. The dataset is important to resolve the ground effect of satellite measurements.


**Specifications Table**

| | |
|---|---|
| Subject area | Air Pollution |
| More specific subject area | Aerosol loading and Retention |
| Type of data | Tableand figure |
| How data was acquired | Multi-angle Imaging Spectro-Radiometer (MISR). |
| Data format | Raw and analyzed |
| Experimental factors | Aerosol Optical Depth |
| Experimental features | Measurement at 550 nm |
| Data source location | Nouakchott-Mauritania |
| Data accessibility | Multi-angle Imaging Spectro-Radiometer |

* Corresponding author.
*E-mail address:* emetere@yahoo.com (M.E. Emetere).

https://doi.org/10.1016/j.dib.2018.07.018

## Value of the data

- The data gives a good background for further study on aerosol loading.
- The data provides technician necessary insight towards configurating sun-photometer over Nouakchott-Mauritania.
- The data helps to quantify the extent of air pollution.
- The data provides modeller necessary insight on aerosol loading and retention challenges over Nouakchott-Mauritania.

## 1. Data

One of the known methods for examining the level of pollution over an area is the aerosol optical depth (AOD). Optical properties of aerosol particles have severe influence over the local radiative forcing and radiation balance of the earth [1,2]. The interaction between aerosol and solar radiation can be described by its optical properties. The optical parameters used to describe the aerosol-solar radiation are the extinction and scattering coefficients, the aerosol depth and the single-scattering phase [3–5]. From the AOD dataset, aerosol hygroscopic growth factor, total atmospheric optical thickness and aerosols loading [6,7].

The primary data was obtained from Multi-angle Imaging Spectro-Radiometer (MISR) i.e. found in Table 1A–1C. The tunning and atmospheric constants for fifteen was obtained using the West African regional scale dispersion model (WASDM) from the AOD dataset (Figs. 2 and 3). The tunning and

**Table 1A**
Summarized aerosol optical depth dataset over Nouakchott.

| Month | 2000 | 2001 | 2002 | 2003 | 2004 | 2005 |
|---|---|---|---|---|---|---|
| **Jan** | 0.8695 | 0.276 | 0.3025 | 0.233833333 | 0.1994 | 0.3684 |
| **Feb** | 0.9052 | 0.36775 | 0.48725 | 0.4885 | 0.384 | 0.392666667 |
| **Mar** | 0.896 | 0.4088 | 0.5454 | 0.4325 | 0.592166667 | 0.2902 |
| **Apr** | 0.70325 | 0.7436 | 0.337 | 0.5725 | 0.552 | 0.6452 |
| **May** | 0.9278 | 0.31325 | 0.528666667 | 0.831666667 | 0.43375 | 0.746333333 |
| **Jun** | 0.9865 | 0.7084 | 0.8676 | 0.8752 | 0.7165 | 0.610833333 |
| **Jul** | 0.781166667 | 0.7262 | 0.90075 | 0.7845 | 0.971333333 | 0.9316 |
| **Aug** | 0.4696 | 0.8254 | 0.7206 | 0.905 | 0.655 | 0.91825 |
| **Sep** | 0.2405 | 0.9795 | 0.753333333 | 0.7454 | 0.6658 | 0.725666667 |
| **Oct** | 0.3702 | 0.5575 | 0.6165 | 0.5506 | 0.445666667 | 0.4772 |
| **Nov** | | 0.4895 | 0.4306 | 0.2888 | 0.37525 | 0.3386 |
| **Dec** | | 0.21075 | 0.2322 | 0.3652 | 0.301833333 | 0.4032 |

**Table 1B**
Summarized aerosol optical depth dataset over Nouakchott.

| Month | 2006 | 2007 | 2008 | 2009 | 2010 |
|---|---|---|---|---|---|
| **Jan** | 0.251 | 0.49375 | 0.463 | 0.2694 | 0.273333333 |
| **Feb** | 0.351333333 | 0.418 | 0.5065 | 0.337 | 0.2435 |
| **Mar** | 0.4844 | 0.3786 | 0.5715 | 0.5065 | 0.6442 |
| **Apr** | 0.770666667 | 0.3885 | 0.9355 | 0.473833333 | 0.6066 |
| **May** | 0.6445 | 0.680833333 | 0.514666667 | 0.7228 | 0.764 |
| **Jun** | 0.8135 | 0.701333333 | 0.6185 | 0.689333333 | 0.673166667 |
| **Jul** | 0.915833333 | 0.8174 | 0.96 | 0.793666667 | 0.947666667 |
| **Aug** | 0.8032 | 0.901333333 | 0.76425 | 0.783 | 0.802833333 |
| **Sep** | 0.6875 | 0.76175 | 0.665333333 | 1.003 | 0.6295 |
| **Oct** | 0.591666667 | 0.5162 | 0.603 | 0.374166667 | 0.36275 |
| **Nov** | 0.2605 | 0.3746 | 0.3645 | 0.25075 | 0.22325 |
| **Dec** | 0.48975 | 0.328166667 | 0.34325 | 0.143333333 | 0.262333333 |

**Table 1C**
Summarized aerosol optical depth dataset over Nouakchott.

| Month | 2011 | 2012 | 2013 |
|---|---|---|---|
| **Jan** | 0.2624 | 0.3988 | 0.5962 |
| **Feb** | 0.243 | 0.28 | 0.2964 |
| **Mar** | 0.2772 | 0.756666667 | 0.2044 |
| **Apr** | 0.647333333 | 0.649666667 | 0.4878 |
| **May** | 0.471 | 0.742333333 | 0.484 |
| **Jun** | 0.588666667 | 0.871666667 | 0.700666667 |
| **Jul** | 0.7044 | 0.762666667 | 0.731 |
| **Aug** | 0.6412 | 0.600833333 | 0.597166667 |
| **Sep** | 0.572 | 0.533833333 | 0.4185 |
| **Oct** | 0.546333333 | 0.25 | 0.3666 |
| **Nov** | 0.284666667 | 0.25875 | 0.175 |
| **Dec** | 0.308 | 0.188 | |

**Table 2**
Atmospheric constants over Nouakchott.

| Location | $a_1$ | $a_2$ | $n_1$ | $n_2$ | $\alpha$ | B |
|---|---|---|---|---|---|---|
| Nouakchott | 0.9442 | 0.8131 | 0.4369 | 0.08213 | $\pm\frac{\pi}{8}$ | $\pm\frac{\pi}{8}$ |


**Fig. 1.** Geographical map of Nouakchott.

atmospheric constants are factors that determines the accuracy of ground instruments e.g. sun photometer [6,7] and they are presented in Table 2. The secondary dataset i.e. aerosol loading was generated using the extended WASDM are presented in Table 3A-C.

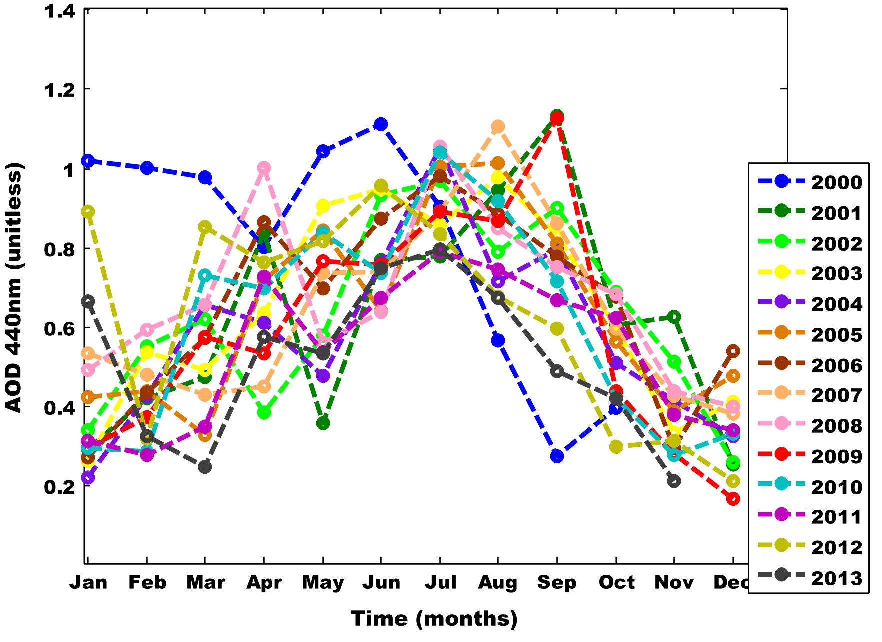


**Fig. 2.** AOD pattern for Nouakchott 2000 – 2013.

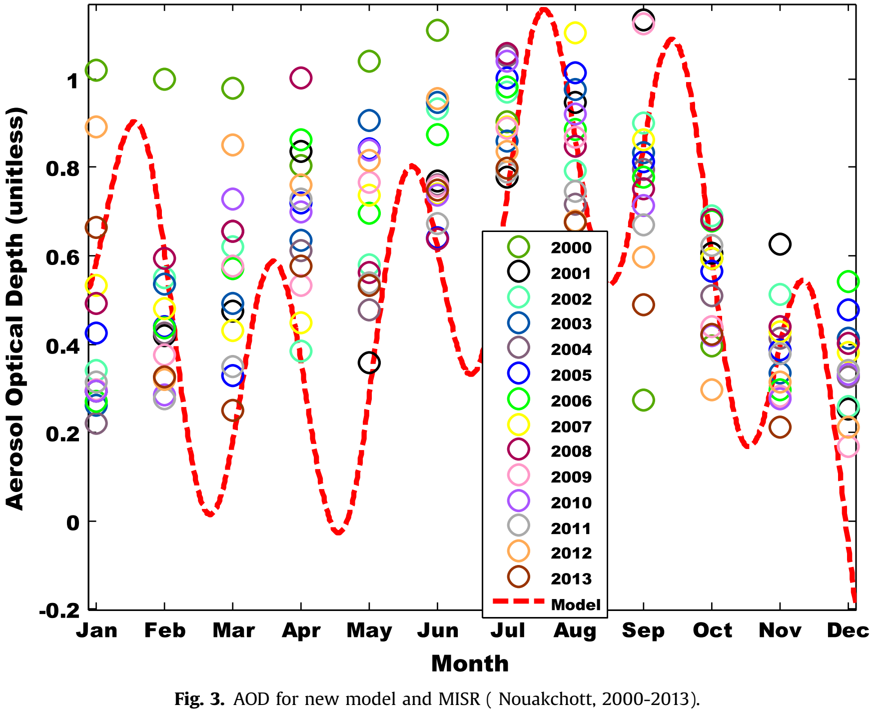


**Fig. 3.** AOD for new model and MISR ( Nouakchott, 2000-2013).

**Table 3A**
Aerosol loading over Nouakchott.

| Month | 2000 | 2001 | 2002 | 2003 | 2004 |
|---|---|---|---|---|---|
| **Jan** | 0.610251849 | 0.859940716 | 0.853678054 | 0.868774357 | 0.874939468 |
| **Feb** | 0.589772356 | 0.83597879 | 0.795581598 | 0.795107337 | 0.831078864 |
| **Mar** | 0.595085002 | 0.823232557 | 0.77245375 | 0.815325887 | 0.752338345 |
| **Apr** | 0.699664467 | 0.679005349 | 0.844718376 | 0.760956028 | 0.76969456 |
| **May** | 0.576626083 | 0.850983355 | 0.779328727 | 0.631523544 | 0.814897949 |
| **Jun** | 0.54192479 | 0.697069678 | 0.611331169 | 0.607007215 | 0.692963222 |
| **Jul** | 0.659127654 | 0.688005495 | 0.592344977 | 0.65733573 | 0.550959607 |
| **Aug** | 0.802167699 | 0.635000181 | 0.690872978 | 0.589888095 | 0.723341959 |
| **Sep** | 0.867471212 | 0.546100116 | 0.673912489 | 0.678066626 | 0.718144143 |
| **Oct** | 0.835252388 | 0.767374939 | 0.741367625 | 0.770282069 | 0.810763945 |
| **Nov** | 0.89151364 | 0.794727189 | 0.815974272 | 0.856983577 | 0.833741237 |
| **Dec** | 0.89151364 | 0.87301247 | 0.869088235 | 0.83673016 | 0.853842252 |

**Table 3B**
Aerosol loading over Nouakchott.

| Month | 2005 | 2006 | 2007 | 2008 | 2009 |
|---|---|---|---|---|---|
| **Jan** | 0.835786501 | 0.865347273 | 0.793104241 | 0.804577017 | 0.861415644 |
| **Feb** | 0.828387115 | 0.84073205 | 0.820210232 | 0.788164773 | 0.844718376 |
| **Mar** | 0.856652431 | 0.796659063 | 0.832728512 | 0.761388138 | 0.788164773 |
| **Apr** | 0.728005794 | 0.664742877 | 0.829688 | 0.572117676 | 0.800606934 |
| **May** | 0.677579322 | 0.728336983 | 0.710809619 | 0.784945797 | 0.689748183 |
| **Jun** | 0.743952326 | 0.641563385 | 0.700626936 | 0.740451104 | 0.706612513 |
| **Jul** | 0.574402948 | 0.583603489 | 0.639418083 | 0.557681382 | 0.652385237 |
| **Aug** | 0.582197336 | 0.647202074 | 0.592008051 | 0.668152109 | 0.658142646 |
| **Sep** | 0.688279207 | 0.707520791 | 0.66947573 | 0.718369984 | 0.532048552 |
| **Oct** | 0.79935715 | 0.75256023 | 0.784336658 | 0.74749559 | 0.834066983 |
| **Nov** | 0.844281011 | 0.863350584 | 0.833936788 | 0.836935581 | 0.865398856 |
| **Dec** | 0.825042825 | 0.794632049 | 0.847098337 | 0.842999029 | 0.882923782 |

**Table 3C**
Aerosol loading over Nouakchott.

| Month | 2010 | 2011 | 2012 | 2013 |
|---|---|---|---|---|
| **Jan** | 0.860540741 | 0.862942723 | 0.826449479 | 0.750543205 |
| **Feb** | 0.866873282 | 0.866973432 | 0.859030287 | 0.855167722 |
| **Mar** | 0.728478842 | 0.859668896 | 0.672158962 | 0.874103366 |
| **Apr** | 0.745871499 | 0.726994853 | 0.725886377 | 0.79537305 |
| **May** | 0.668284589 | 0.801652868 | 0.679665079 | 0.796809857 |
| **Jun** | 0.714564347 | 0.753888506 | 0.609019683 | 0.700961295 |
| **Jul** | 0.56496546 | 0.699086143 | 0.668990707 | 0.685536266 |
| **Aug** | 0.647402069 | 0.729894787 | 0.748469507 | 0.750111577 |
| **Sep** | 0.735370769 | 0.761172157 | 0.777224566 | 0.820044262 |
| **Oct** | 0.837447557 | 0.772065182 | 0.865553311 | 0.836318235 |
| **Nov** | 0.870770385 | 0.857952393 | 0.863723734 | 0.878729234 |
| **Dec** | 0.862957082 | 0.852310418 | 0.876770215 | 0.89151364 |

## 2. Experimental design, materials and methods

Mauritania is located on latitude 16°N to 22°N and longitude 7°W to 17°W. It is bounded within an approximate total area of 1,030,700 $km^2$. Its geographical structure includes arid plains, cliff, plateau and oases. Its climate is hot with irregular rainfall. Nouakchott is located on longitude and latitude of 18.09° and $-15.98$° (Fig. 1).

**Table 4**
Percentage of increase of aerosols loading over Nouakchott.

| **Year** | 2001 | 2004 | 2007 | 2009 |
|---|---|---|---|---|
| Percentage (%) | 29.1 | 3.6 | 4.7 | 8.0 |

The West African regional scale dispersion model (WASDM) for calculating aerosol loading over a region:

$$\psi(\lambda) = a_1{}^2 \cos\left(\frac{\mathrm{n}_1\pi\tau(\lambda)}{2}x\right)\cos\left(\frac{\mathrm{n}_1\pi\tau(\lambda)}{2}y\right) + \ldots\ldots a_n{}^2 \cos\left(\frac{\mathrm{n}_\mathrm{n}\pi\tau(\lambda)}{2}x\right)\cos\left(\frac{\mathrm{n}_\mathrm{n}\pi\tau(\lambda)}{2}y\right) \quad (1)$$

a is atmospheric constant gotten from the fifteen years aerosol optical depth (AOD) dataset from MISR, $n$ is the tunning constant, $\tau(\lambda)$ is the AOD of the area and $\psi(\lambda)$ is the aerosol loading. The analysis of Eq. (1) was done using the C++ codes.

The value of the atmospheric and tuning constant for fifteen years was determine using Eq. (1) over fifteen years data (Figs. 1 and 2). The summary of the AOD is shown in Table 1. The value atmospheric and tuning constant i.e. obtained from the comprehensive dataset is shown in Table 2 . The secondary dataset i.e. aerosol loading was generated using the extended WASDM are presented in Table 3A–3C. The percentage of the highest aerosol loading is shown in Table 4.

## Acknowledgement

The authors appreciate Covenant University for partial sponsorship. The authors acknowledge NASA for primary dataset. Emetere M.E. enjoys partial sponsorship from University of Johannesburg as Senior Research Associates.

## Transparency document. Supporting information

Transparency data associated with this article can be found in the online version at https://doi.org/10.1016/j.dib.2018.07.018.

## References

[1] K. Vijayakumar, P.C.S. Devara, Study of aerosol optical depth, ozone, and precipitable water vapour content over Sinhagad, a high-altitude station in the Western Ghats, Int. J. Remote Sens. 34 (2) (2013) 613–630.
[2] O. Boucher, J. Quaas, Water vapour affects both rain and aerosol optical depth, Nat. Geosci. 6 (2013) 4–5.
[3] J.-J. Cao, C.-S. Zhu, X.-X. Tie, F.-H. Geng, H.-M. Xu, S.S.H. Ho, G.-H. Wang, Y.-M. Han, K.-F. Ho, Characteristics and sources of carbonaceous aerosols from Shanghai, China, Atmos. Chem. Phys. 13 (2013) 803–817.
[4] Y. Yang, H. Liao, S.-J. Lou, Simulated impacts of sulphate and nitrate aerosol formation on surface-layer ozone concentrations in China, Atmos. Ocean. Sci. Lett. 7 (5) (2014) 441–446.
[5] D.F. Zhao, A. Buchhol, B. Kortner, P. Schlag, F. Rubach, H. Fuchs, A. Kiendler-Scharr, R. Tillmann, A. Wahner, Å.K. Watne, M. Hallquist, J.M. Flores, Y. Rudich, K. Kristensen, A.M.K. Hansen, M. Glasius, I. Kourtchev, M. Kalberer, T.F. Mentel, Cloud condensation nuclei activity, droplet growth kinetics and hygroscopicity of biogenic and anthropogenic Secondary Organic Aerosol (SOA), Atmos. Chem. Phys. Discuss. 15 (2015) 19903–19945.
[6] M.E. Emetere, M.L. Akinyemi, O. Akinojo, Parametric retrieval model for estimating aerosol size distribution via the AERONET, LAGOS station, Environ. Pollut. 207 (C) (2015) 381–390.
[7] E. Emetere Moses, M.L. Akinyemi, T.E. Oladimeji, Statistical examination of the aerosols loading over Kano-Nigeria: the satellite observation analysis, Sci. Rev. Eng. Environ. Sci. 72 (2016) 167–176.